Electronic Supplementary Information

Enhancement of H_2 Adsorption in Li^+-Exchanged Co-ordination Framework Materials

Sihai Yang,[1] Xiang Lin,[1] Alexander J. Blake,[1] K. Mark Thomas,[2] Peter Hubberstey,[1] Neil R. Champness[1]* and Martin Schröder[1]*

1. School of Chemistry, University of Nottingham, University Park, NG7 2RD, UK.

2. Northern Carbon Research Laboratories. Sir Joseph Swan Institute for Energy Research and School of Chemical Engineering and Advanced Materials, University of Newcastle upon Tyne, Newcastle upon Tyne, NE1 7RU, UK.

1. Experimental section

1.1 Materials and Measurements.

All reagents and solvents were used as received from commercial suppliers without further purification. Analyses for C, H, and N were carried out on a CE-440 elemental analyzer. Thermal gravimetric analyses (TGA) were performed under nitrogen atmosphere (60 ml/min) with a heating rate of 2 °C/min using a TA SDT-600 thermogravimetric analyzer. IR spectra were recorded using a Nicolet Avatar 360 FT-IR spectrophotometer, and analyses for Li and In were carried out on ICP-OES analyzer. Calibration curves for ICP-OES were prepared by dilution of commercially available standards with the sample dissolved in concentrated HNO_3, and diluted to proper concentration for measurement. Powder X-ray diffraction (PXRD) data were collected over the 2θ range 5-50^o on a Philips X'pert diffractometer using Cu Kα radiation (λ = 1.5418 Å) at 40 kV and 40mA.

1.2 Synthesis of $Me_2NH_2[In(L)].(DMF).(CH_3CN).(H_2O)_4$ (1) and $Li_{0.5}(H_3O)_{0.5}[In(L)].(H_2O)_5.(C_3H_6O)_{0.5}$ (1-Li).

H_4L[1] (0.015 g, 0.05 mmol) and $In(NO_3)_3$ (0.0137 g, 0.05 mmol) were mixed and dispersed in a mixture of DMF/acetonitrile (1.5 ml, 2:1 v/v). The resulting white slurry turned clear upon addition of two drops of 6M HNO_3 solution. The solution was then heated to 90°C for 1 day and the colorless crystalline product separated by filtration and washed sequentially by DMF, and dried in air. Yield: 0.08 g (70%). To prepare the Li^+-doped sample, crystals of as-synthesized **1** were immersed in concentrated solution of LiCl in distilled water/acetone (v/v=1/1). The crystals were soaked for ten days, and the solvent was refreshed everyday. Upon decanting the metal chloride solutions, the cation-exchanged crystals of **1-Li**$^+$ were rinsed and soaked in distilled water/acetone (v/v=1/1) for 3 days to remove residual free LiCl within the pores of **1-Li**$^+$. Elemental analysis (% calc/found): for **1**, $InO_{13}C_{23}H_{32}N_3$ (C 41.0/39.0, H 4.8/4.4, N 6.3/7.1); for **1-Li**$^+$, $InO_{14}C_{17.5}H_{20.5}Li_{0.5}$ (C 36.6/34.9, H 3.6/2.9, N 0.0/0.0). The volatility of crystallization solvents in the samples contributes to the discrepancy in elemental analytical data. Selected IR: for **1**, ν = 3443(w),

2926(w), 1650(vs), 1569(m), 1490(w), 1410(s), 1384(vs), 1253(m), 1094(m), 1060(m), 907(w), 856(w), 773(m), 747(s), 659(m); for **1-Li**$^+$, 3469(w), 2927(w), 1703(m), 1612(m), 1552(m), 1418(s), 1364(vs), 1229(m), 1090(m), 992(m), 913(w), 782(m), 710(m), 657(m).

1.3 X-ray Crystallographic Study.

The data for **1** were collected on Station 9.8 of the Synchrotron Radiation Source at STFC Daresbury Laboratory. The details for data collection are included in CIF files in Supplementary Information. Structures were solved by direct methods and developed by difference Fourier techniques using the SHELXTL software package.[1] The hydrogen atoms on the ligand were placed geometrically and refined using a riding model. The unit cell volume includes a large region of disordered solvent which could not be modelled as discrete atomic sites. We employed PLATON/SQUEEZE[2] to calculate the contribution to the diffraction from the solvent region and thereby produced a set of solvent-free diffraction intensities. The final formula was calculated from the SQUEEZE[2] results combined with elemental analysis data and TGA data.

† Crystal data for **1**: $[In(C_{16}H_6O_8)(CH_3)_2NH_2]\cdot(C_3H_7NO)\cdot(CH_3CN)\cdot(H_2O)_4$, M = 673.34, tetragonal, space group $I4_1/acd$, $a = b$ = 19.659(3), c = 36.149(7) Å, V = 13971(4), Z = 16, T = 120(2) K, μ = 0.732 mm^{-1}, 48568 reflections measured, 3088 unique (R_{int} = 0.066) which were used in all calculations. Final R_1 = 0.0602 [2393 $F > 4\sigma(F)$], wR_2 [all F^2] = 0.183, maximum ΔF peak 0.67 eÅ^{-3}. The unit cell includes a large region of disordered solvent which could not be modelled as discrete atomic sites. We employed PLATON/SQUEEZE[2] to calculate the contribution to the diffraction from the solvent region and thereby produced a set of solvent-free diffraction intensities. The final formula was calculated from the SQUEEZE results combined with elemental analysis data and TGA data: the contents of the solvent region are therefore represented in the unit cell contents but are not included in the refinement model.

1.4 Nitrogen and Hydrogen adsorption isotherms.

N_2 and H_2 isotherms were recorded on a IGA system (Hiden Isochema, Warrington, UK) at the University of Nottingham under ultra high vacuum in a clean system with a diaphragm and turbo pumping system. Ultra-pure plus grade (99.9995%) H_2 was purchased from BOC and purified further using calcium aluminosilicate and activated carbon adsorbents to remove trace amounts of water and other impurities before introduction into the IGA system. The density of H_2 at 78 K in the buoyancy correction was calculated by the Redlich-Kwong-Soave equation of state of H_2 incorporated in the IGASWIN software of the IGA system.

2. X-ray crystal structure for 1.

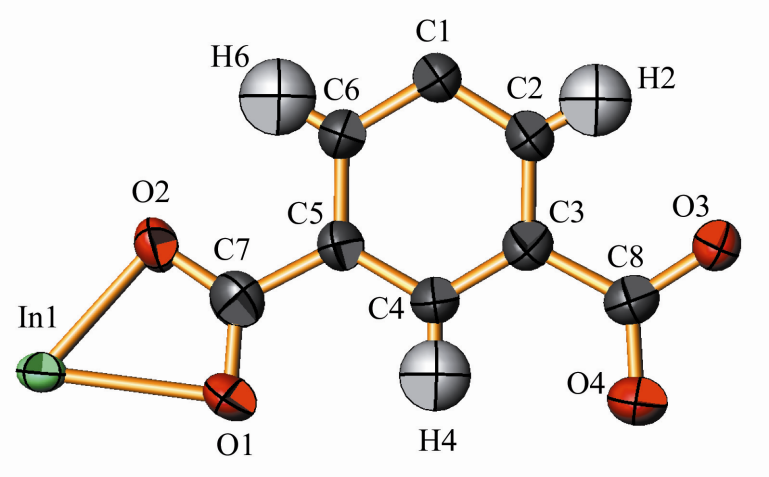

Figure 1s: View of the asymmetric unit for **1**.

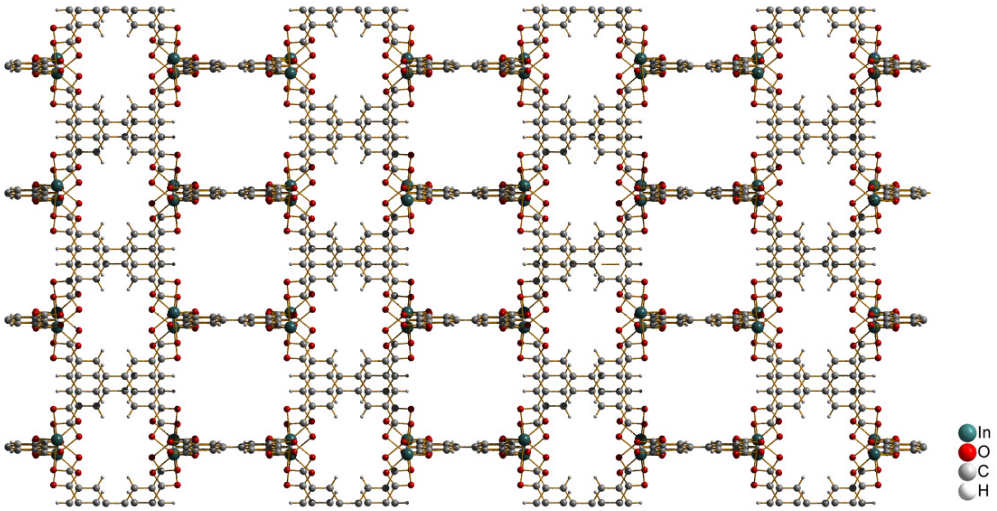

Figure 2s: View of **1** along the crystallographic *a*-axis.

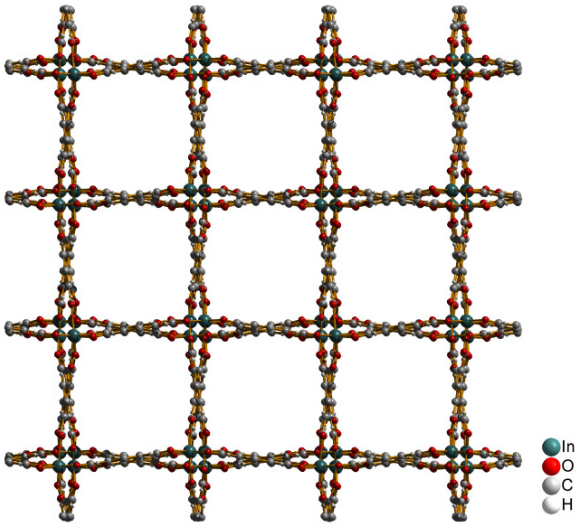

Figure 3s: View of **1** along the crystallographic *c*-axis.

3. TGA plots for 1 and 1-Li$^+$.

1 and **1-Li**$^+$ show very similar thermal stability (Figure 4s). The weight loss of 26.0% from **1** correlates with solvent loss based upon one DMF, one CH_3CN, and four water molecules per indium (calc. 27.6 wt%). The solvent loss of 22.4% from **1-Li**$^+$ correlates to half a molecule of acetone and 5.5 molecules of water per indium (calc. 24.9 wt%). The volatility of crystallization solvents in the samples contributes to the discrepancies between room temperature and 300°C. This

is attributable to small losses of volatile solvent during procedures of loading and weighing of samples. After Li^+-cation exchange, the guest solvent CH_3CN and DMF are replaced by acetone and water. As a result, the solvent in **1-Li**$^+$ is more readily lost during the heat treatment.

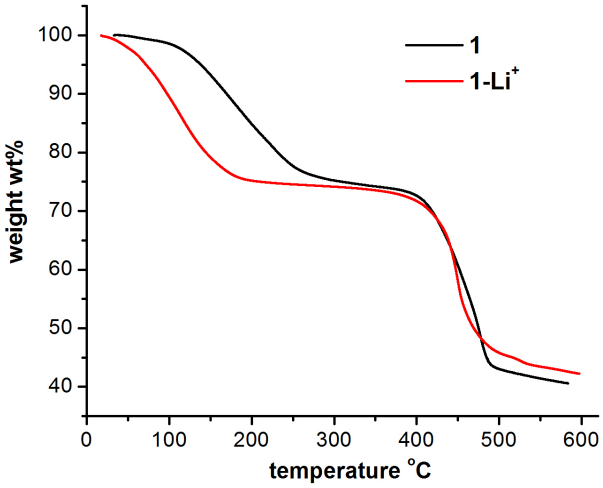

Figure 4s TGA plots for **1** and **1-Li**$^+$.

3. IR Spectra

The IR spectrum of **1-Li**$^+$ (Figure 5s) showed a broad peak between 3700 and 3100 cm^{-1}, suggesting the presence of the guest water molecule which may be co-ordinated to Li$^+$ in the pores. However, no peak was found at the same region in the spectrum for desolvated **1a-Li**$^+$, indicating that it is possible to remove completely the water coordinated to Li$^+$. Comparison of IR spectra between **1** and desolvated **1a** shows that the guest water molecules in the pore of **1** can also be removed.

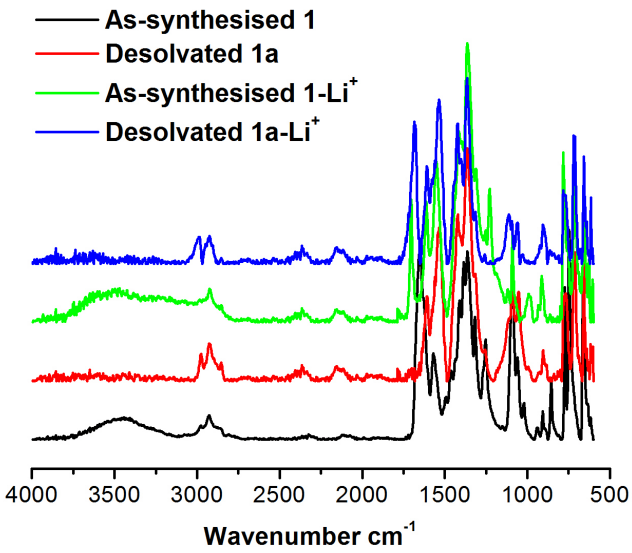

Figure 5s: IR spectra for as-synthesised **1** and **1-Li** and desolvated **1a** and **1a-Li**$^+$.

3. Powder X-Ray diffraction

Powder X-ray diffraction confirms the purity of bulk samples of **1** (Figure 6s) and that the framework **1** persists in acetone-solvent-exchanged **1** and desolvated **1a (**Figure 7s). Comparison of the PXRD traces of **1** and **1-Li**$^+$ clearly shows no new peaks or shifting of peaks, suggesting that the structure of framework remains intact after Li^+ exchange (Figure 8s). The desolvated **1a-Li**$^+$ was also stable in air but will take up water from the atmosphere.

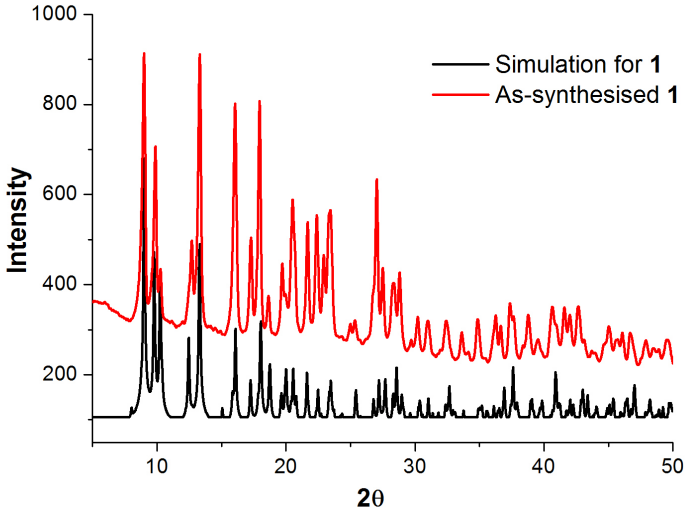

Figure 6s: PXRD patterns for **1**.

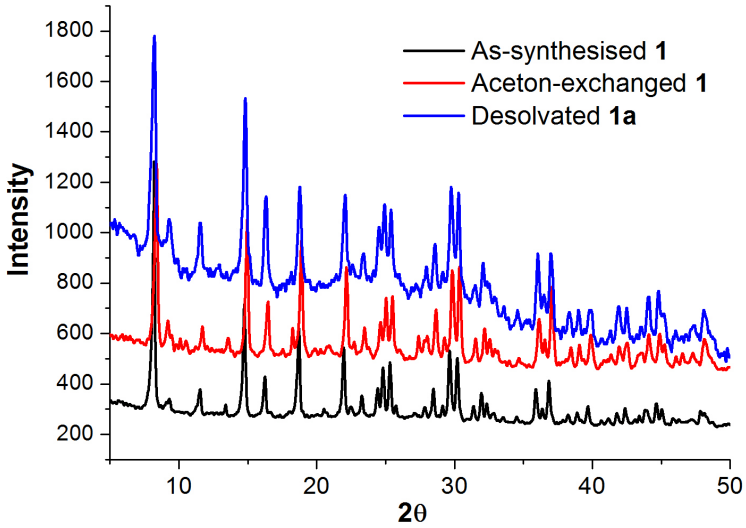

Figure 7s: PXRD patterns for as-synthesized **1**, acetone solvent exchanged **1**, and desolvated **1a**.

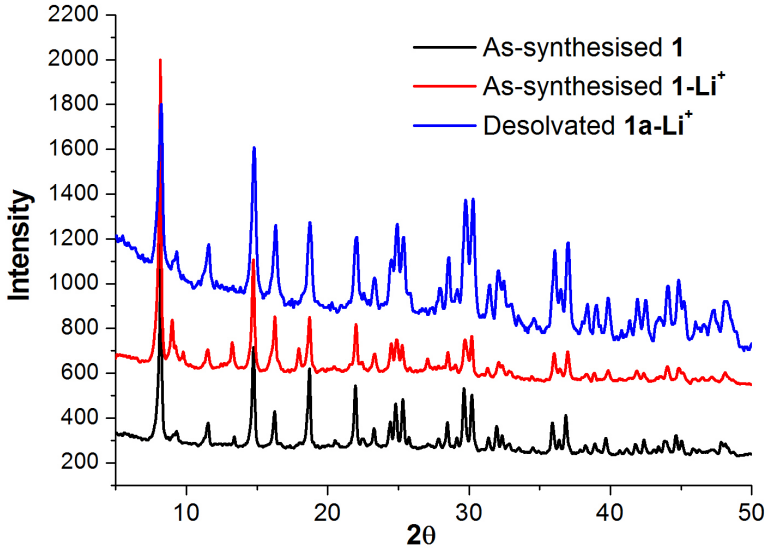

Figure 8s: PXRD patterns for as-synthesized **1** and **1-Li**$^+$, and desolvated **1a-Li**$^+$.

6. Adsorption Enthalpy simulation for 1a and 1a-Li$^+$:

Gravimetric H_2 adsorption data were recorded over the range 0-20 bar at both 78 K and 88 K for **1** and **1-Li**$^+$. All data were rigorously corrected for the buoyancy of the system, samples and absorbates. All H_2 isotherms show good reversibility and an absence of hysteresis (Figures 9s and 10s). The H_2 adsorption kinetic data confirm that equilibrium is achieved rapidly within *ca*. 3 mins of the isotherm pressure step. These suggest a typical H_2 adsorption and exclude any significant effect due to the presence of impurities

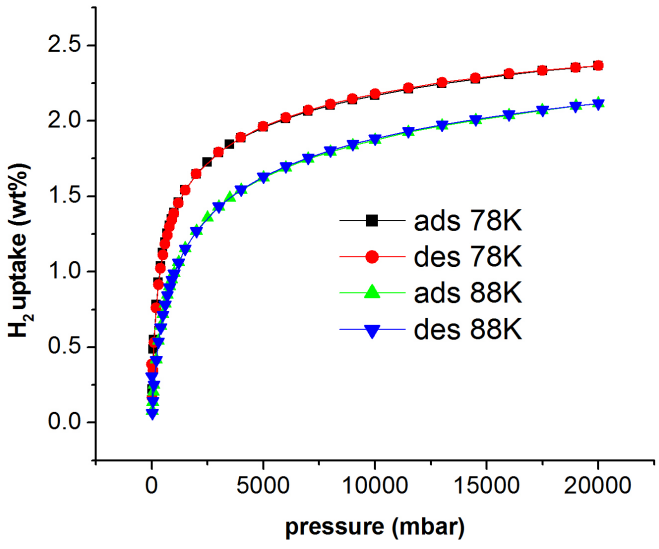

Figure 9s: H_2 isotherms for **1a** at 78 K and 88 K.

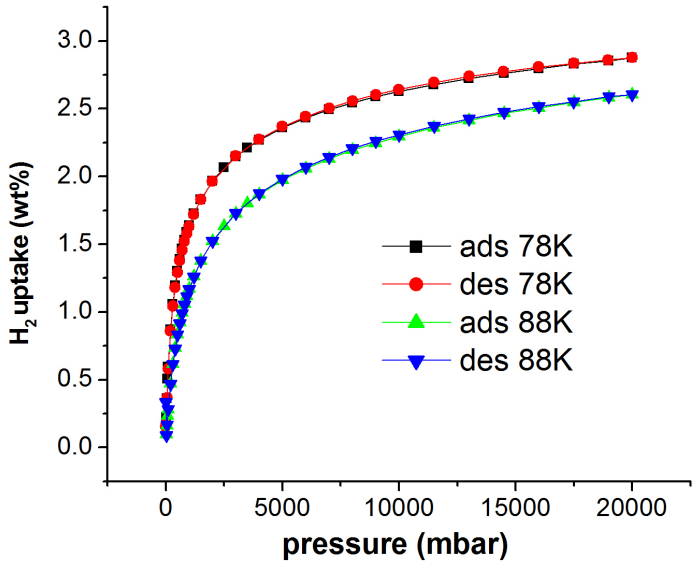

Figure 10s: H_2 isotherms for **1a-Li**$^+$ at 78 K and 88 K.

The isosteric heats of adsorption Q_{st} were determined by fitting a virial-type equation to both the 78 K and 88 K H_2 adsorption isotherms. The *ln(p)* values for a given amount adsorbed (*n*) were calculated from the linear regressions determined from the virial equation analysis using the following virial equation.[3-9]

$$\ln(n/p) = A_0 + A_1 n + A_2 n^2 ..... \qquad (1)$$

where *p* is pressure, *n* is amount adsorbed and A_0, A_1 etc. are virial coefficients. A_0 is related to adsorbate-adsorbent interactions, whereas A_1 describes adsorbate-adsorbate interactions.[5] Henry's Law constant (K_H) is equal to $\exp(A_0)$, and at low surface coverage, A_2 and higher terms can be neglected. Therefore, a graph of $\ln(n/p)$ versus *n* should give a straight line at low surface coverage. This approach has been used for analysis of adsorption of a wide range of gases[5-9], including hydrogen,[3,4] on a variety of adsorbents.

The simulation data for H_2 adsorption at 78 and 88 K for **1a** between 50-400 mbar using equation (1) are shown in Figures 11s and 12s. The simulation data for H_2 adsorption at 78 and 88 K by equation (1) on **1a-Li**$^+$ are shown in Figures 13s and 14s. All the regression coefficients were larger than 0.999, confirming that the model fits the data very well. The A_1 virial parameters for **1a** and **1a-Li**$^+$ at 78 K are low -300.9, -224.8 g mol^{-1}, respectively, as shown in Figures 11s and 13s.

This means that the H_2–H_2 interactions are lower for **1a-Li**$^+$ in line with the decrease in enthalpy. This reflects the increase in pore size on going from **1a** to **1a-Li**$^+$. Similar values have been obtained for hydrogen adsorption on activated carbons.[3,4] The A_1 virial parameters of **1a** and **1a-Li**$^+$ for 88 K are lower, -229.2, -196.9 g mol^{-1}, respectively, than at 78K (Figures 12s and 14s). This has also been observed for hydrogen adsorption on M'MOF**1**, [10] and is thus consistent previous studies of virial parameters for H_2 and D_2 adsorption.

The virial method based on equation (1) is preferred at low pressure because the linearity in the low pressure part of the isotherm provides direct confirmation of the accuracy of the interpolations. Also, the intercept of the graph gives A_0, where the Henry's Law constant $K_H = \exp(A_0)$ and this is a measure of the H_2 surface interaction. The isosteric enthalpies for H_2 adsorption on **1a** and **1a-Li**$^+$ were calculated as a function of surface coverage. We estimate the error in the measured isosteric enthalpies as 0.1 kJ/mol.

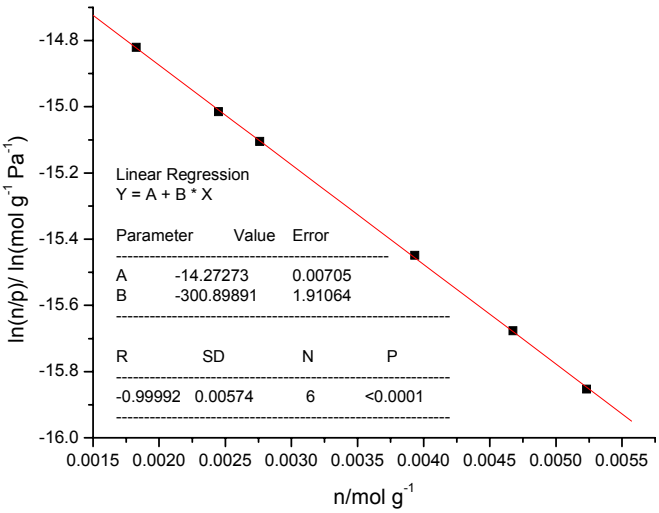

Figure 11s: Virial plot for the adsorption of H_2 on **1a** at 78 K.

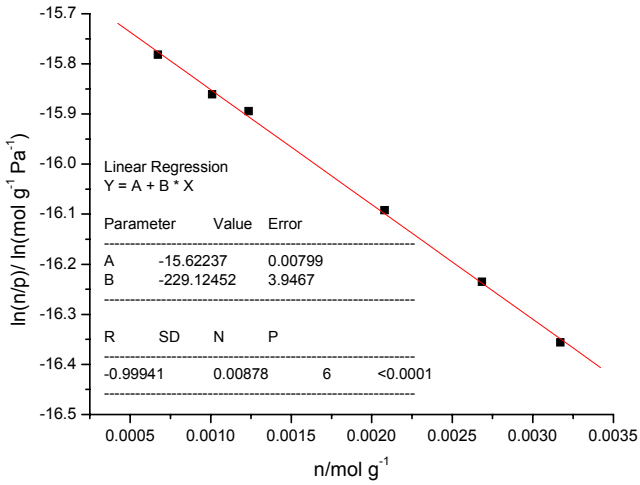

Figure 12s: Virial plot for the adsorption of H_2 on **1a** at 88 K.

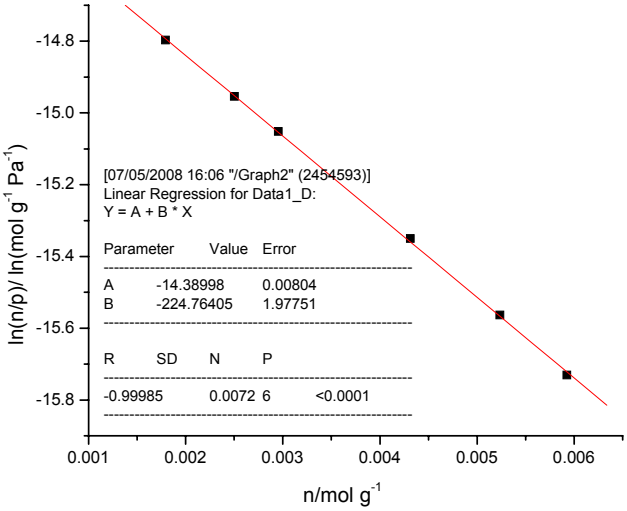

Figure 13s: Virial plot for the adsorption of H_2 on **1a-Li**$^+$ at 78 K.

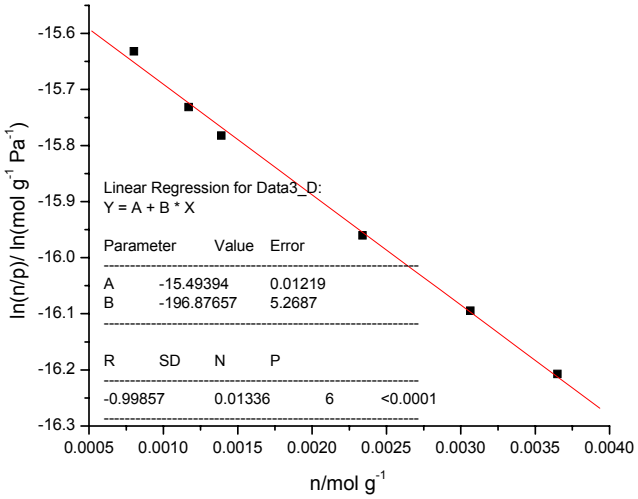

Figure 14s: Virial plot for the adsorption of H_2 on **1a-Li**$^+$ at 88 K.

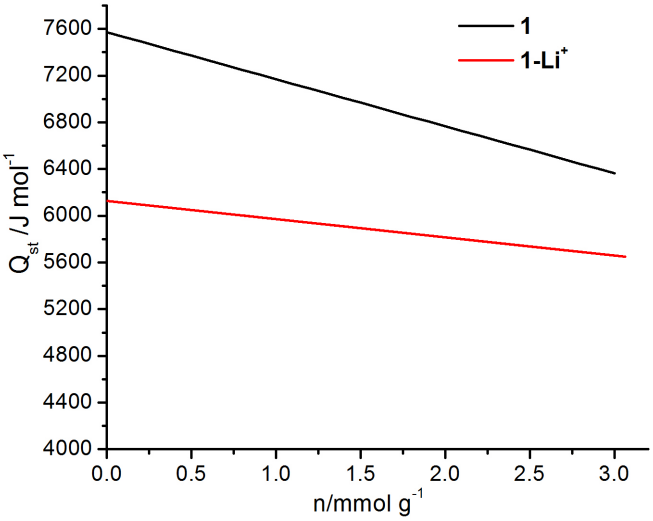

Figure 15s: Isosteric heat of H_2 adsorption for **1a** and **1a-Li**$^+$ at low surface coverage.

Table 1 Physical characteristics and sorption properties of **1a** and **1a-Li**$^+$.

Sample	**1a**	**1a-Li**$^+$
Formula (desolvated)	$[In(L)](CH_3)_2NH_2$	$[In(L)]Li_{0.5}H_{0.5}$
Maximum N_2 uptake (ml/g)	210.0	269.4
BET surface area (m^2/g)	820	1024
Evacuated framework density (g/cm^3)	0.9267	0.8466
Accessible void (%)[a]	69	69
Pore volume (N_2) (cm^3/g)	0.326	0.419
Pore size (N_2) (Å)	5.8	7.0
H_2 uptake (1 bar/20 bar) (wt%)	1.39/2.36	1.66/2.88
Maximum uptake from Langmuir-Freundlich plot (wt%)	2.72	3.27
Adsorbed H_2 density at 20 bar (g/cm^3)[b]	0.0724	0.0687
Maximum H_2 uptake in volumetric unit (g/L)	25.2	27.7
Maximum adsorption enthalpy at zero surface coverage (kJ/mol)	7.57	6.13

[a] from PLATON/SOLV[2], and the contribution of organic cations has been neglected; [b] calculation with pore volume from maximum N_2 uptake.

Reference:

1. G. M. Sheldrick, *Acta Crystallogr. Section A,* 2008, **64**, 112.
2. A. L. Spek, *J. Appl. Crystallogr.* 2003, **36**, 7; P. v.d. Sluis and A. L. Spek, *Acta Crystallogr*., *Sect. A*, 1990, **46**, 194.
3. X. Zhao, S. Villar-Rodil, A. J. Fletcher and K. M. Thomas, *J. Phys Chem. B,* 2006, **110**, 9947.
4. X. Zhao, B. Xiao, A. J. Fletcher and K. M. Thomas, *J. Phys. Chem B,* 2005, **109**, 8880.
5. J. H. Cole, D. H. Everett, C. T. Marshall, A. R. Paniego, J. C. Powl and F. Rodriguez-Reinoso, *J. Chem. Soc. Faraday Trans,* 1974,**70**, 2154.
6. I. P. O'Koye, M. Benham and K. M. Thomas, *Langmuir* 1997, **13**, 4054.
7. C. R. Reid, I. P. O'Koye and K. M. Thomas, *Langmuir* 1998, **14**, 2415.
8. C. R. Reid and K. M. Thomas, *Langmuir* 1999, **15**, 3206.
9. C. R. Reid and K. M. Thomas, *J. Phys. Chem. B* 2001, **105**, 10619.
10. B. Chen, X. Zhao, A. Putkham, K. Hong, E. B. Lobkovsky, E. J. Hurtado, A. J. Fletcher and K. M. Thomas, *J. Am. Chem. Soc.* 2008, **130**, 6411.